Journal of Southeast University (English Edition) Vol. 27, No. 1, pp. 40 – 46 Mar. 2011 ISSN 1003—7985

Load spectrum analysis for combined frame of closed high-speed press

Zheng Enlai Jia Fang Zhang Zhisheng Shi Jinfei

(School of Mechanical Engineering, Southeast University, Nanjing 211189, China)

Abstract: Based on the basic theory of mechanics, kinematic and dynamic analysis for a slider-crank mechanism with a balance mechanism is performed. The theoretical formula of the load spectrum for the interaction between the crank shaft and the bearing seat of the upper beam is achieved by approximately simplifying the mechanical model of the crank shaft. The simulation for the load spectrum data of combined frame under the operating conditions of blanking or piling is performed using Matlab and the law of the load spectrum curves under these two conditions is analyzed. The simulation results show that under a no-load condition, the load spectrum curves of the interaction between the crank shaft and the bearing seat of the upper beam present a form of periodic sine wave and under the piling condition, the load spectrum curves of the interaction between the crank shaft and the bearing seat of the upper beam present a form of periodic pulse wave. The simulation results can provide a theoretical foundation for the load determination during the process of analyzing the dynamic characteristics on the combined frame of a closed high-speed press through the finite element method.

Key words: press; load spectrum; crank shaft; slider-crank mechanism

doi: 10.3969/j.issn.1003 – 7985.2011.01.009

The vibration of high-speed press is mainly caused by the inertia force produced during the rotation of the crank shaft and the blow force under blanking operating conditions. In order to perform a dynamic analysis on the combined frame of closed high-speed press more accurately through the finite element method, the determination of the load spectrum for the interaction between the crank shaft and the bearing seat of the upper beam is particularly important and will directly determine the accuracy of the dynamic analysis for the combined frame. The determination of a load spectrum between the crank shaft and the bearing seat of the upper beam is mainly focused on the dynamic analysis of the crank-slider transmission mechanism for the closed high-speed press.

A considerable amount of research on the dynamics of the crank-slider mechanism has been performed by domestic and foreign scholars and a great number of significant achievements have been made. Based on the rigid body dynamics theory, Hahn et al.[1-3] studied the dynamic characteristics of a single-point-driven press by the computer simulation method and simulation results of three different complicated mathematical models for the press are in good agreement with experimental data. Lieh[4] presented the model and a dynamic analysis of a slider-crank mechanism with flexible joints and couplers and formulated the equations of motion of the mechanism using a newly evolved multibody formalism and cast in terms of a minimum set of generalized coordinates through a Jacobian matrix expansion. Mukras et al.[5] established the model of a coupling between joint wear and system kinematics of the crank-slider mechanism by integrating a wear prediction process and built a widely used finite-element-based iterative scheme. Three different modeling techniques are presented based on different assumptions, and their performances are compared in terms of joint force and wear depths. According to the problems of dynamic unbalance and vibration caused by considering linkage as a fixed lumped mass during the process of dynamic analyzing on the press, Lee[6] proposed the variable lumped mass impact theory to solve the problem of dynamic analysis and design. Due to the imbalance problem of lateral inertia force on the closed crank press, Zhang et al.[7-8] proposed a kind of symmetrical layout structure for the slider-crank mechanism, of which the dynamic model is built by ADAMS and dynamic inertia force is tested and analyzed using the post processing module of ADAMS. Yao[9] and Lin[10] obtained the expression of inertia force to perform kinematic and dynamic analysis for the slider-crank mechanism without a balance mechanism.

As far as we know, no attempts have been reported about the theoretical method to determine the load spectrum for the interaction between the crank shaft and the bearing seat of the upper beam. The kinematic and dynamic analysis for the slider-crank mechanism with a balance mechanism using the theory of mechanics is performed in this paper, and the theoretical formula of the load spectrum is achieved by simplifying the crank as a simply supported beam with a statically indeterminate structure. The law of the load spectrum under two kinds of conditions is analyzed by simulation.

1 Physical Description

The closed high-speed press, as shown in Fig. 1, is a type of forging machine using a mechanical drive. Motion with energy from the motor are transmitted to the working mechanism through the transmission system, which make the blank achieve a certain deformation to obtain needed work pieces. The working principle is shown in Fig. 2. The belt transmits the motion of the motor from the small pulley to the big pulley, then the motion is transmitted on the crank shaft from the big pulley. The upper end of the main linkage is installed on the crank shaft and the lower end is installed to the slider, which converts the rotary motion of the crank shaft into the straight reciprocating motion. In order to balance the inertia force, additional weight is set up

Received 2010-11-22.

Biographies: Zheng Enlai(1986—), male, graduate; Jia Fang (corresponding author), female, doctor, associate professor, 13851896116@139.com.

Foundation items: The Key Technologies R&D Program of Jiangsu Province (No. BE2006036), Transformation Program of Science and Technology Achievements of Jiangsu Province (No. BA2008030).

Citation: Zheng Enlai, Jia Fang, Zhang Zhisheng, et al. Load spectrum analysis for combined frame of closed high-speed press[J]. Journal of Southeast University (English Edition), 2011, 27(1): 40 – 46. [doi: 10.3969/j.issn.1003 – 7985.2011.01.009]

at the other end of the crank shaft. To meet the needs of the production process, the slider alternates motion and motionless so the brake and clutch are installed on the press. The working time of the press with load is fairly short during a whole action cycle and most of the action cycle is free motion time without load. The crank shaft press often has a fly wheel to keep the load-bearing of the motor uniform and makes use of the energy effectively. The big pulley shown in Fig. 1 also acts as a fly wheel.

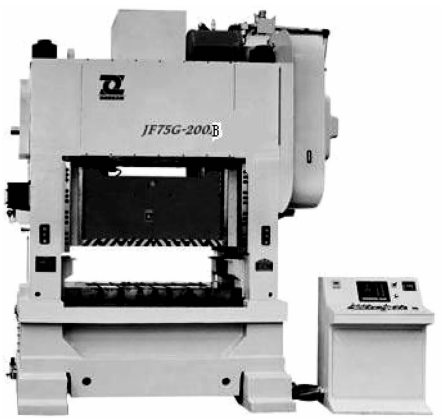

Fig. 1 Physical figure of closed high-speed press

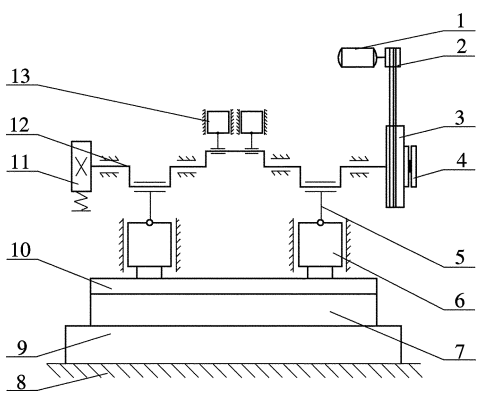

1—Motor; 2—Motor wheel; 3—Fly wheel; 4—Clutch; 5—Linkage 6—Slider; 7—Lower die; 8—Foundation; 9—Worktable; 10—Upper die 11—Brake; 12—Crank; 13—Additional weight

Fig. 2 Composition and principle sketch of press

2 Kinematic Analysis

For the closed high-speed press, its executive mechanism is a slider-crank mechanism with a balance mechanism, which includes four linkages in total (two main linkages and two auxiliary linkages). For the sake of convenience, the motion relationship sketch is simplified as shown in Fig. 3.

Taking B_0 and F_0 as the starting points of the displacement of slider S_3 and the displacement of additional weight S_6, as shown in Fig. 3, the relationship between the displacement of slider S_3, the displacement of additional weight S_6 and the angle of the crank shaft can be expressed as

$$\left.\begin{aligned} S_3 &= (R_1 + L_1) - (R_1\cos\alpha + L_1\cos\beta) \\ S_6 &= (R_2 + L_2) - (R_2\cos\alpha + L_2\cos\gamma) \end{aligned}\right\} \tag{1}$$

From the geometric relationship, we obtain

$$R_1\sin\beta = L_1\sin\alpha,\ R_2\sin\gamma = L_2\sin\alpha \tag{2}$$

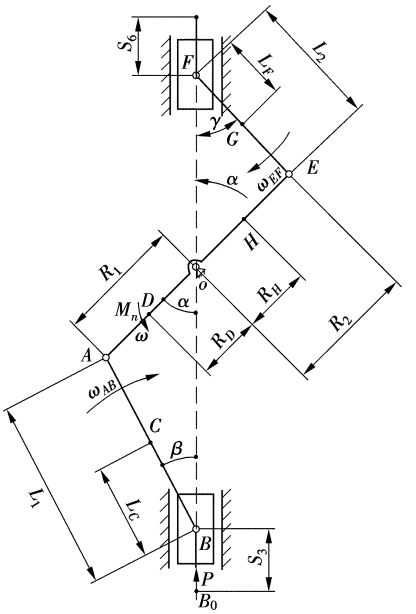

Fig. 3 Motion sketch of slider-crank mechanism

Set $\lambda_1 = R_1/L_1$, $\lambda_2 = R_2/L_2$, then

$$\sin\beta = \lambda_1\sin\alpha,\ \sin\gamma = \lambda_2\sin\alpha \tag{3}$$

Then

$$\left.\begin{aligned} \cos\beta &= \sqrt{1-\sin^2\beta} = \sqrt{1-\lambda_1^2\sin^2\alpha} \\ \cos\gamma &= \sqrt{1-\sin^2\gamma} = \sqrt{1-\lambda_2^2\sin^2\alpha} \end{aligned}\right\} \tag{4}$$

Expand according to the Taylor series, and take the first two terms,

$$\left.\begin{aligned} \sqrt{1-\lambda_1^2\sin^2\alpha} &\approx 1-\frac{1}{2}\lambda_1^2\sin^2\alpha \\ \sqrt{1-\lambda_2^2\sin^2\alpha} &\approx 1-\frac{1}{2}\lambda_2^2\sin^2\alpha \end{aligned}\right\} \tag{5}$$

Then the relationship between the displacement of slider S_3, the displacement of additional weight S_6 and the angle of the crank shaft can also be expressed as

$$\left.\begin{aligned} S_3 &= R_1\left[(1-\cos\alpha) + \frac{\lambda_1}{4}(1-\cos 2\alpha)\right] \\ S_6 &= R_2\left[(1-\cos\alpha) + \frac{\lambda_2}{4}(1-\cos 2\alpha)\right] \end{aligned}\right\} \tag{6}$$

By the derivation of displacements, the velocity expression can be achieved,

$$\left.\begin{aligned} v_3 &= \frac{\mathrm{d}s_3}{\mathrm{d}t} = \frac{\mathrm{d}s_3}{\mathrm{d}\alpha}\frac{\mathrm{d}\alpha}{\mathrm{d}t} = \omega R_1\left(\sin\alpha + \frac{\lambda_1}{2}\sin 2\alpha\right) \\ v_6 &= \frac{\mathrm{d}s_6}{\mathrm{d}t} = \frac{\mathrm{d}s_6}{\mathrm{d}\alpha}\frac{\mathrm{d}\alpha}{\mathrm{d}t} = \omega R_2\left(\sin\alpha + \frac{\lambda_2}{2}\sin 2\alpha\right) \end{aligned}\right\} \tag{7}$$

By the derivation of velocities, the acceleration expression can be achieved,

$$\left.\begin{aligned} a_3 &= \frac{\mathrm{d}v_3}{\mathrm{d}t} = \omega^2 R_1(\cos\alpha + \lambda_1\cos 2\alpha) \\ a_6 &= \frac{\mathrm{d}v_6}{\mathrm{d}t} = \omega^2 R_2(\cos\alpha + \lambda_2\cos 2\alpha) \end{aligned}\right\} \tag{8}$$

While the crank shaft is rotating, the main linkage and auxiliary linkage move in planar complex motion, and the slider and additional weight move in translation motion. Decompose the motion of the main linkage into two parts: the translation of the slider and the rotation of hinge point B. Decompose the motion of the auxiliary linkage into two parts: the translation of the additional weight and hinge point F. Set the rate of turning of the main linkage as ω_{AB} relative to the slider, and set the rate of turning of the auxiliary linkage as ω_{EF} relative to the additional weight. Because the slider and the additional weight only move in translation motion, ω_{AB} and ω_{EF} are the absolute ratings of turning of the main linkage and the auxiliary linkage, respectively. Because $\beta = \omega_{AB}t$, $\gamma = \omega_{EF}t$, $\sin\beta = \lambda_1 \sin\alpha$, $\sin\gamma = \lambda_2 \sin\alpha$, we can obtain

$$\omega_{AB}\cos\beta = \lambda_1\omega\cos\alpha,\ \omega_{EF}\cos\gamma = \lambda_2\omega\cos\alpha \tag{9}$$

$$\omega_{AB} = \frac{\lambda_1\omega\cos\alpha}{\cos\beta},\ \omega_{EF} = \frac{\lambda_2\omega\cos\alpha}{\cos\gamma} \tag{10}$$

Because λ_1, λ_2 are much less than 0.3, and

$$\left.\begin{aligned}\cos\beta &= 1 - \frac{1}{2}\lambda_1^2\sin^2\alpha \approx 1\\ \cos\gamma &= 1 - \frac{1}{2}\lambda_2^2\sin^2\alpha \approx 1\end{aligned}\right\} \tag{11}$$

We can obtain

$$\omega_{AB} = \lambda_1\omega\cos\alpha,\ \omega_{EF} = \lambda_2\omega\cos\alpha \tag{12}$$

As the main linkage moves in translation motion relative to the slider as well as swinging around point B of the slider and the auxiliary linkage moves in translation motion relative to the additional weight as well as swinging around point F of the additional weight, the acceleration of center C of mass has three components a_3, a_{2n}, $a_{2\tau}$ and the acceleration of center G of mass also has three components a_6, a_{5n}, $a_{5\tau}$. The normal acceleration and tangential acceleration can be expressed as

$$\left.\begin{aligned}a_{2n} &= L_C\omega_{AB}^2 = \lambda_1^2\omega^2 L_C\cos\alpha\\ a_{2\tau} &= L_C\frac{\mathrm{d}\omega_{AB}}{\mathrm{d}t} = -\lambda_1\omega^2 L_C\sin\alpha\end{aligned}\right\} \tag{13}$$

$$\left.\begin{aligned}a_{5n} &= L_F\omega_{EF}^2 = \lambda_2^2\omega^2 L_F\cos\alpha\\ a_{5\tau} &= L_F\frac{\mathrm{d}\omega_{EF}}{\mathrm{d}t} = -\lambda_2\omega^2 L_F\sin\alpha\end{aligned}\right\} \tag{14}$$

The main crank shaft and the auxiliary crank shaft rotate with a constant angular velocity ω, so the centripetal acceleration a_1, a_4 for mass center D of the main crank shaft and mass center H of the auxiliary crank shaft are expressed as

$$a_1 = R_D\omega^2,\ a_4 = R_H\omega^2 \tag{15}$$

3 Dynamic Analysis

According to the d'Alembert principle, the inertia force, active force and constraint force acting on a motion system form a balance force system. Through the center-of-mass motion theorem, the force sketch of the slider-crank mechanism is shown in Fig. 4 (All the friction resistances are ignored).

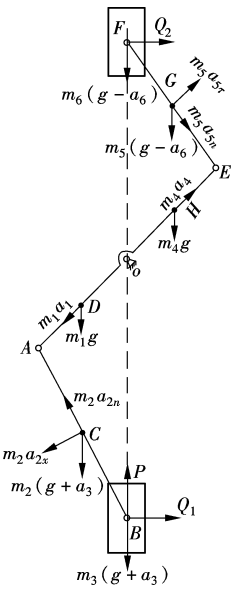

Fig. 4 Force sketch of slider-crank mechanism

First, analyzing the forces acting on the main linkage and separating the main linkage, the force sketch of the main linkage is shown in Fig. 5(a), in which F_{A1}, F_{A2} are forces acting on the main linkage by the main crank shaft.

Due to $\lambda_1 < 0.3$, we can generally consider $\cos\beta \approx 1$ for the sake of convenience. According to the force balance relationship of the main linkage, we obtain

$$\left.\begin{aligned}F_{A1} &= (m_2 + m_3)(g + a_3) - P - m_2a_{2n} +\\ &\quad m_2a_{2\tau}\lambda_1\left(1 - \frac{L_C}{L_1}\right)\sin\alpha +\\ &\quad \lambda_1^2\sin^2\alpha\left[(g + a_3)\left(m_2 + m_3 - m_2\frac{L_C}{L_1}\right) - P\right]\\ F_{A2} &= m_2a_{2\tau}\frac{L_C}{L_1} + m_2(a_3 + g)\lambda_1\frac{L_C}{L_1}\sin\alpha\\ Q_1 &= m_2a_{2\tau}\left(1 - \frac{L_C}{L_1}\right) +\\ &\quad \lambda_1\sin\alpha\left[(g + a_3)\left(m_2 + m_3 - m_2\frac{L_C}{L_1}\right) - P\right]\end{aligned}\right\} \tag{16}$$

Separating the auxiliary linkage to analyze the force acting on the auxiliary linkage, the force sketch of the auxiliary is shown in Fig. 5(b), in which F_{E1}, F_{E2} are forces acting on the auxiliary linkage by the auxiliary crank shaft.

According to the force balance relationship of the auxiliary linkage, we obtain

$$\left.\begin{aligned}F_{E1} &= (m_5 + m_6)(g - a_6) + m_5a_{5n} + \lambda_2^2\sin^2\alpha(g - a_6)\cdot\\ &\quad \left(m_5 + m_6 - m_5\frac{L_F}{L_2}\right) - m_5a_{5\tau}\lambda_2\left(1 - \frac{L_F}{L_2}\right)\sin\alpha\\ F_{E2} &= m_5a_{5\tau}\frac{L_F}{L_2} - m_5(g - a_6)\lambda_2\frac{L_F}{L_2}\sin\alpha\\ Q_2 &= \lambda_2\sin\alpha(g - a_6)\left(m_5 + m_6 - m_5\frac{L_F}{L_2}\right) - m_5a_{5\tau}\left(1 - \frac{L_F}{L_2}\right)\end{aligned}\right\} \tag{17}$$

Finally, separating the main crank shaft and the auxiliary crank shaft to analyze the forces, the force sketch of the main crank shaft and the auxiliary crank shaft is shown in Fig. 5(c).

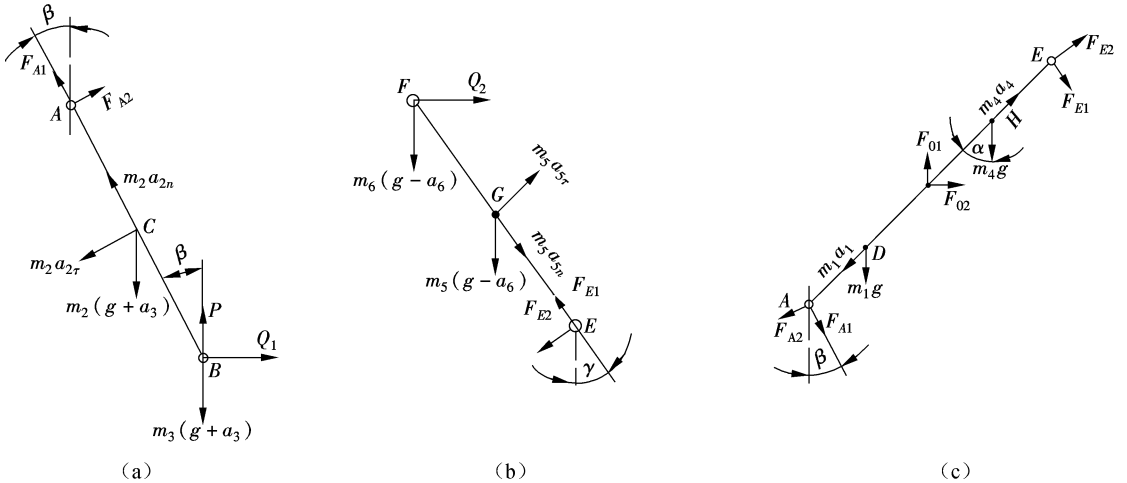

Fig. 5 Force sketch of main crank shaft and auxiliary. (a) Main linkage; (b) Auxiliary linkage; (c) Main and auxiliary crank shaft

Therefore, the support reaction force of the crank shaft is derived as

$$\left.\begin{aligned} F_{01} &= m_1a_1\cos\alpha + m_1g + F_{A1} + F_{A2}\lambda_1\sin\alpha + \\ &\quad m_4g - m_4a_4\cos\alpha + F_{E1}\lambda_2\sin\alpha - F_{E2} \\ F_{02} &= F_{A1}\lambda_1\sin\alpha - F_{A2} + m_1a_1\sin\alpha - \\ &\quad m_4a_4\sin\alpha - F_{E1} - F_{E2}\lambda_2\sin\alpha \end{aligned}\right\} \quad (18)$$

4 Theoretical Formula of Load Spectrum

The schematic diagram for the support structure of the crank shaft is shown in Fig. 6 and the crank shaft can be simplified to the force model shown in Fig. 7. Then the constrained force of the four bearing pedestals can be obtained.

Removing the constraints, the force model can be obtained. The force model is a symmetrical statically indeterminate structure. Taking half of the model into consideration, the statically indeterminate force model of the crank shaft can be achieved as shown in Fig. 8.

According to the force sketch of the main crank shaft and auxiliary crank shaft as shown in Fig. 7, we obtain

$$\left.\begin{aligned} F_{Ax} &= a\sin\beta - b\cos\beta - m_1a_1\sin\alpha \\ F_{Ay} &= -(a\cos\beta + b\sin\beta) - m_1g - m_1a_1\cos\alpha \end{aligned}\right\} \quad (19)$$

$$\left.\begin{aligned} F_{Ex} &= c\sin\gamma + d\cos\gamma + m_4a_4\sin\alpha \\ F_{Ey} &= d\sin\gamma - c\cos\gamma + m_4a_4\cos\alpha - m_4g \end{aligned}\right\} \quad (20)$$

where

$$\begin{aligned} a &= (m_2+m_3)(g+\omega^2R_1(\cos\alpha+\lambda_1\cos2\alpha)) - P - m_2\lambda_1^2\omega^2L_C\cos\alpha - m_2\lambda_1\omega^2L_C\sin\alpha\lambda_1(1-L_C/L_1)\sin\alpha + \\ &\quad \lambda_1^2\sin^2\alpha[(g+\omega^2R_1(\cos\alpha+\lambda_1\cos2\alpha))(m_2+m_3-m_2L_C/L_1) - P] \\ b &= -m_2\lambda_1\omega^2L_C\sin\alpha L_C/L_1 + m_2(\omega^2R_1(\cos\alpha+\lambda_1\cos2\alpha)+g)\lambda_1L_C/L_1\sin\alpha \\ c &= (m_5+m_6)(g-\omega^2R_2(\cos\alpha+\lambda_2\cos2\alpha)) + m_5\lambda_2^2\omega^2L_F\cos\alpha - m_5\lambda_2\omega^2L_F\sin\alpha\lambda_2(1-L_F/L_2)\sin\alpha + \\ &\quad \lambda_2^2\sin^2\alpha(g-\omega^2R_2(\cos\alpha+\lambda_2\cos2\alpha))(m_5+m_6-m_5L_F/L_2) \\ d &= -m_5\lambda_2\omega^2L_F\sin\alpha L_F/L_2 - m_5(g-\omega^2R_2(\cos\alpha+\lambda_2\cos2\alpha))\lambda_2L_F/L_2\sin\alpha \end{aligned}$$

The deflections of points M and N under the action of F_{Mx}, F_{My} are

$$\left.\begin{aligned} \Delta_{Mx}^{(F_{Mx})} &= -F_{Mx}(L_3+L_4)^3/(3EI) \\ \Delta_{My}^{(F_{My})} &= -F_{My}(L_3+L_4)^3/(3EI) \\ \Delta_{Nx}^{(F_{Mx})} &= -F_{Mx}L_2^2(3L_3+3L_4-L_2)/(6EI) \\ \Delta_{Ny}^{(F_{My})} &= -F_{My}L_2^2(3L_3+3L_4-L_2)/(6EI) \end{aligned}\right\} \quad (21)$$

The deflections of points M and N under the action of F_{Ax}, F_{Ay} are

$$\left.\begin{aligned} \Delta_{Mx}^{(F_{Ax})} &= F_{Ax}L_3^2(2L_3+3L_4)/(6EI) \\ \Delta_{My}^{(F_{Ay})} &= F_{Ay}L_3^2(2L_3+3L_4)/(6EI) \\ \Delta_{Nx}^{(F_{Ax})} &= F_{Ax}L_2^2(3L_3-L_2)/(6EI) \\ \Delta_{Ny}^{(F_{Ay})} &= F_{Ay}L_2^2(3L_3-L_2)/(6EI) \end{aligned}\right\} \quad (22)$$

The deflections of points M and N under the action of F_{Nx}, F_{Ny} are

$$\left.\begin{aligned} \Delta_{Mx}^{(F_{Nx})} &= -F_{Nx}L_2^2(3L_3+3L_4-L_2)/(6EI) \\ \Delta_{My}^{(F_{Ny})} &= -F_{Ny}L_2^2(3L_3+3L_4-L_2)/(6EI) \\ \Delta_{Nx}^{(F_{Nx})} &= -F_{Nx}L_2^3/(3EI) \\ \Delta_{Ny}^{(F_{Ny})} &= -F_{Ny}L_2^3/(3EI) \end{aligned}\right\} \quad (23)$$

The deflections of points M and N under the action of F_{Ex}, F_{Ey} are

$$\left.\begin{aligned} \Delta_{Mx}^{(F_{Ex})} &= F_{Ex}L_1^2(3L_3+3L_4-L_1)/(6EI) \\ \Delta_{My}^{(F_{Ey})} &= F_{Ey}L_1^2(3L_3+3L_4-L_1)/(6EI) \\ \Delta_{Nx}^{(F_{Ex})} &= F_{Ex}L_1^2(3L_2-L_1)/(6EI) \\ \Delta_{Ny}^{(F_{Ey})} &= F_{Ey}L_1^2(3L_2-L_1)/(6EI) \end{aligned}\right\} \quad (24)$$

As points M and N are constrained, therefore,

$$\left.\begin{aligned} \Delta_{Mx} &= \Delta_{Mx}^{(F_{Mx})} + \Delta_{Mx}^{(F_{Ax})} + \Delta_{Mx}^{(F_{Nx})} + \Delta_{Mx}^{(F_{Ex})} = 0 \\ \Delta_{My} &= \Delta_{My}^{(F_{My})} + \Delta_{My}^{(F_{Ay})} + \Delta_{My}^{(F_{Ny})} + \Delta_{My}^{(F_{Ey})} = 0 \\ \Delta_{Nx} &= \Delta_{Nx}^{(F_{Mx})} + \Delta_{Nx}^{(F_{Ax})} + \Delta_{Nx}^{(F_{Nx})} + \Delta_{Nx}^{(F_{Ex})} = 0 \\ \Delta_{Ny} &= \Delta_{Ny}^{(F_{My})} + \Delta_{Ny}^{(F_{Ay})} + \Delta_{Ny}^{(F_{Ny})} + \Delta_{Ny}^{(F_{Ey})} = 0 \end{aligned}\right\} \quad (25)$$

By solving the above equations, we obtain

$$\left.\begin{aligned}
F_{Nx} &= -\{[2(3L_3 - L_2)(L_3 + L_4)^3 - L_3^2(2L_3 + 3L_4)(3L_3 + 3L_4 - L_2)]F_{Ax} + L_1^2[2(3L_2 - L_1)(L_3 + L_4)^3 - \\
&\quad (3L_3 + 3L_4 - L_1)(3L_3 + 3L_4 - L_2)L_2^2]F_{Ex}\}/[L_2^2(3L_3 + 3L_4 - L_2)^2 - 4L_2(L_3 + L_4)^3] \\
F_{Ny} &= -\{[2(3L_3 - L_2)(L_3 + L_4)^3 - L_3^2(2L_3 + 3L_4)(3L_3 + 3L_4 - L_2)]F_{Ay} + L_1^2[2(3L_2 - L_1)(L_3 + L_4)^3 - \\
&\quad (3L_3 + 3L_4 - L_1)(3L_3 + 3L_4 - L_2)L_2^2]F_{Ey}\}/[L_2^2(3L_3 + 3L_4 - L_2)^2 - 4L_2(L_3 + L_4)^3] \\
F_{Mx} &= (3L_3 - L_2)F_{Ax} - 2L_2F_{Nx} + L_1^2/L_2^2(3L_2 - L_1)F_{Ex} \\
F_{My} &= (3L_3 - L_2)F_{Ay} - 2L_2F_{Ny} + L_1^2/L_2^2(3L_2 - L_1)F_{Ey}
\end{aligned}\right\} \quad (26)$$

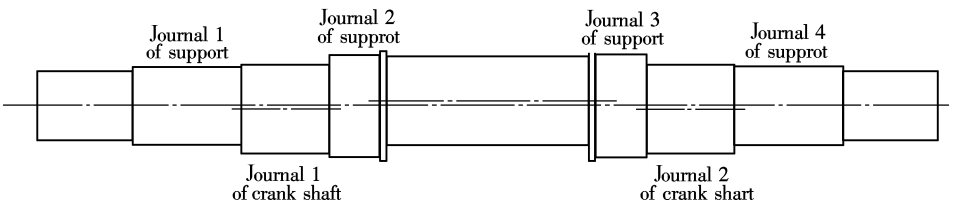

Fig. 6 Schematic diagram for support structure of crank shaft

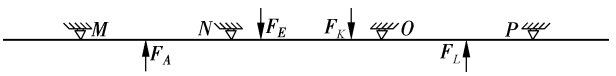

Fig. 7 Statically indeterminate force model of crank shaft

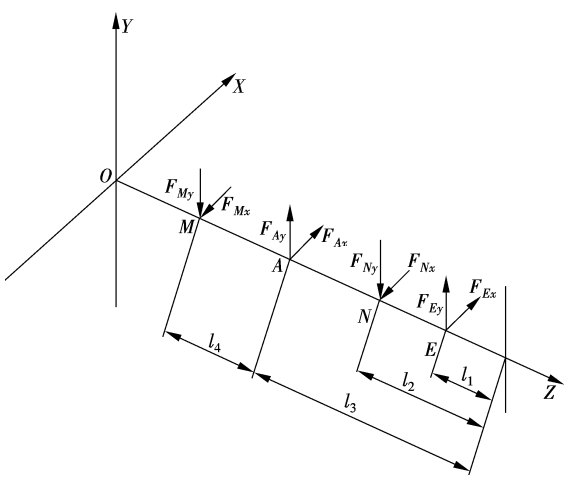

Fig. 8 Statically indeterminate force model of crank shaft

5 Numerical Simulation

Take JF75G-200 press as an example and the parameters of the slider-crank mechanism are shown in Tab. 1.

Tab. 1 Lists of parameters for slider-crank mechanism

Parameter	Value	Parameter	Value
L_F/mm	310	R_1/mm	15
L_C/mm	412	R_2/mm	25
L_1/mm	485	m_1/kg	0
L_2/mm	460	m_2/kg	270
l_1/mm	165	m_3/kg	2 180
l_2/mm	325.5	m_4/kg	0
l_3/mm	495	m_5/kg	70
l_4/mm	184	m_6/kg	1 360

When the piling force is zero (That means no-load condition), we obtain the theoretical load spectrum data under a no-load condition as shown in Fig. 9 and Fig. 10 by substituting the parameters in Tab. 1 into the theoretical load spectrum formula.

As shown in Fig. 9 and Fig. 10, under a no-load condition, the load spectrum curves of the interaction between the crank shaft and the bearing seat of the upper beam present a form of periodic sine wave. According to Fig. 9 and Fig. 10, the average value for the load spectrum of point N along the y direction is -13.339 kN, and the amplitude is 11.461 kN. The average value for the load spectrum of point M along the y direction is 8 N, and the amplitude is 4.286 kN. The average value for the load spectrum of point N along the x direction is -11.150 kN, and the amplitude is 4.286 kN. The average value for the load spectrum of point M along the x direction is 2 N, and the amplitude is 3.275 kN.

When the piling force is 120 t, the theoretical load spectrum curves under the piling condition can be achieved as shown in Fig. 11 and Fig. 12.

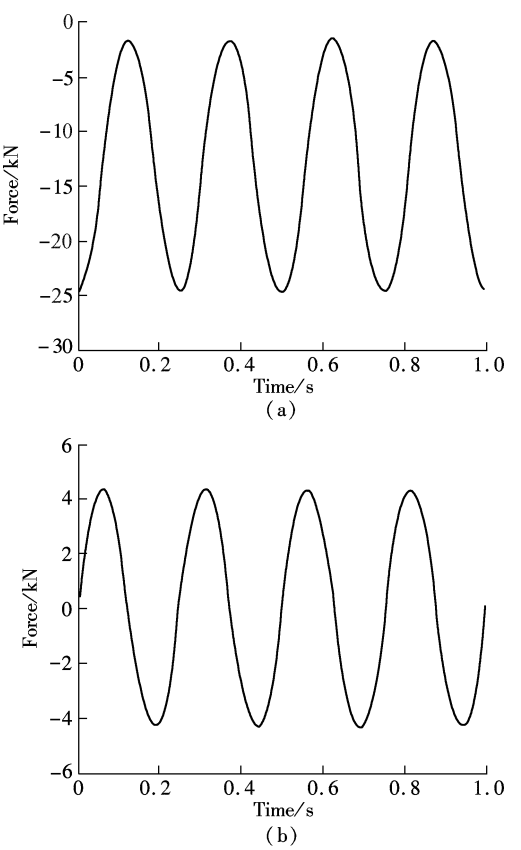

Fig. 9 Load spectrum of points N and M along y direction. (a) Load spectrum of point N; (b) Load spectrum of point M

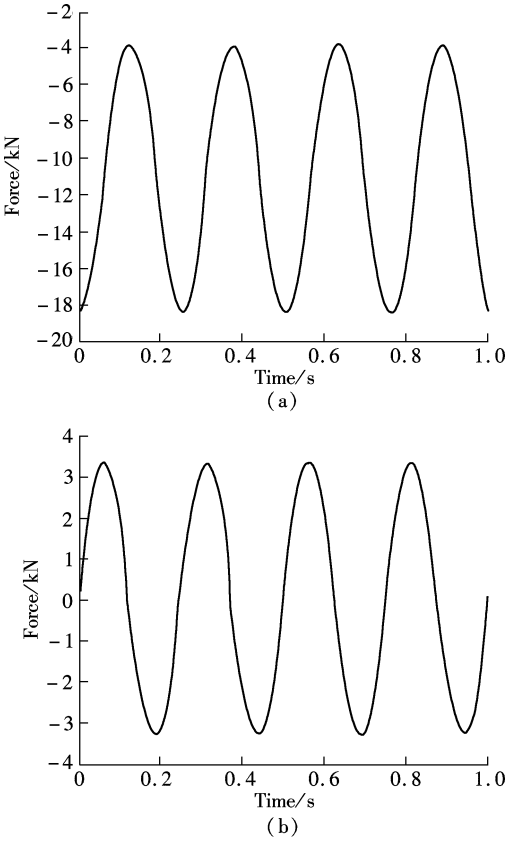

Fig. 10 Load spectrum of points N and M along x direction. (a) Load spectrum of point N; (b) Load spectrum of point M

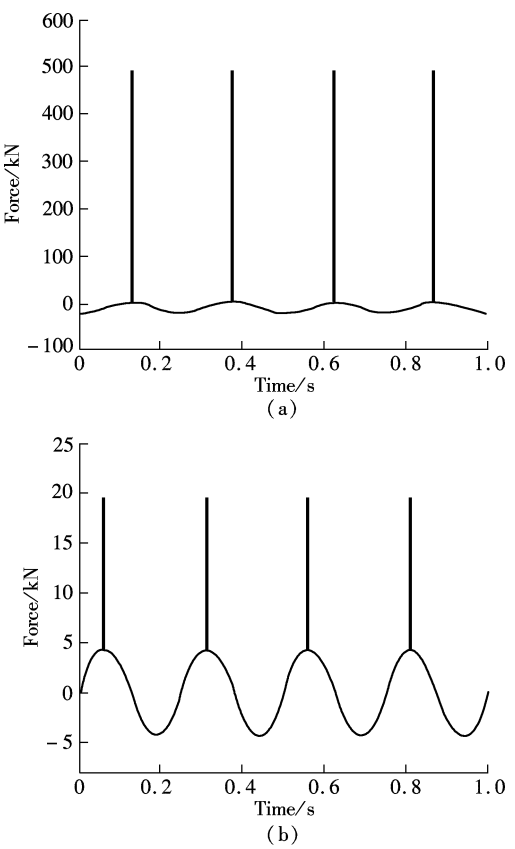

Fig. 11 Load spectrum of points N and M along y direction. (a) Load spectrum of point N; (b) Load spectrum of point M

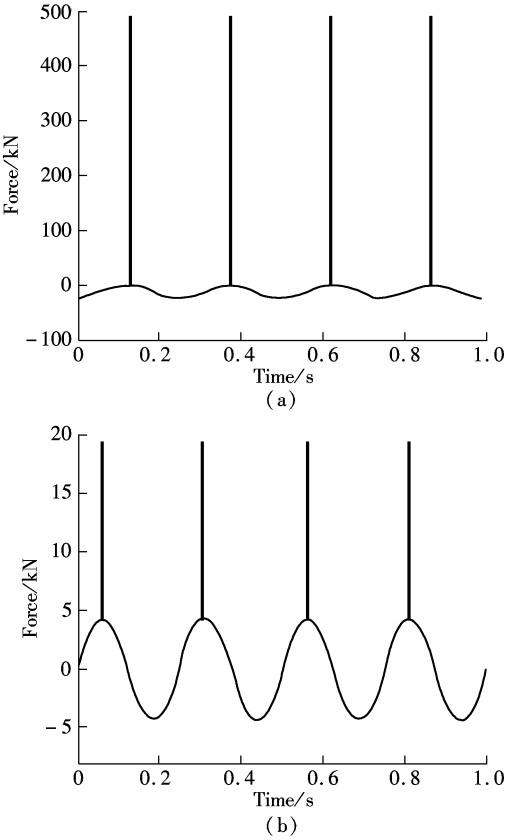

Fig. 12 Load spectrum of points N and M along x direction. (a) Load spectrum of point N; (b) Load spectrum of point M

As shown in Fig. 11 and Fig. 12, under the piling condition, the load spectrum curves of the interaction between the crank shaft and the bearing seat of the upper beam present a form of periodic pulse waves because of the giant impact produced at the striking instant of up-piling and down-piling. When the up-piling and the down-piling is out of contact, the load spectrum presents the form of a periodic sine wave, which is mainly caused by the inertia force of the slider-crank mechanism. The peak value of point N along the y direction is 487.6 kN, and the peak value of point M along the y direction is 373.2 kN. The peak value of point N along the x direction is 19.44 kN, and the peak value of point M along the x direction is 14.5 kN.

6 Conclusion

Based on the theory of mechanics, kinematic and dynamic analysis for a slider-crank mechanism with a balance mechanism is performed in this paper, and the theoretical formula of the load spectrum for the interaction between the crank shaft and the bearing seat of the upper beam is achieved by simplifying the crank as a statically indeterminate, simply supported beam. By simulating the load spectrum curve under no-load and piling conditions using Matlab, the law of the load spectrum curve can be explored. The simulation results can be provided for the load determination during the process of analyzing the dynamic performance on the combined frame of a high-speed press through the finite element method.

References

[1] Hahn H. Mathematische modelle masseloser gelenke zur simulation räumlicher bewegungen von Starrkopersystemen [R]. Kassel: Department of Mechanical Engineering of Kassel University, 1988.

[2] Wagener H W, Neumann M. Rechnergestutzte analyse des dynamischen verhaltens mechanischer pressen [R]. Kassel: Department of Mechanical Engineering of Kassel University, 1997.

[3] Neumann M, Hahn H. Computer simulation and dynamic analysis of a mechanical press based on different engineer models [J]. *Mathematics and Computers in Simulation*, 1998, **46**(5): 559 - 574.

[4] Lieh Junghsen. Dynamic modeling of a slider-crank mechanism with coupler and joint flexibility [J]. *Mechanism and Machine Theory*, 1994, **29**(1): 139 - 147.

[5] Mukras S, Mauntler N, Kim N H, et al. Dynamic modeling of a slider-crank mechanism under joint wear [C]// *Proceedings of the* 32*nd Annual Mechanism and Robotics Conference*. New York, 2008: 443 - 452.

[6] Lee H J. Dynamics and probabilistic fatigue analysis schemes for high-speed press machines [J]. *Computers and Structures*, 1994, **55**(1): 11 - 19.

[7] Zhang Xiaoyang, Wang Xingsong, Jia Fang, et al. Dynamic balance optimization on high speed crank press [J]. *Forging and Stamping Technology*, 2006, **31**(6): 94 - 99.

[8] Mao Jun, Zhang Xiaoyang. Study on the dynamic balance optimization of high speed crank press [J]. *Journal of Jinling Institute of Technology*, 2007, **23**(4): 4 - 9. (in Chinese)

[9] Yao Yan. *Elastodynamic research and computer simulation of high-speed press* [D]. Xi'an: Mechanical Engineering of Xi'an University of Technology, 2007. (in Chinese)

[10] Lin Haiou. *Vibration research of high speed press and computer simulation* [D]. Xi'an: Mechanical Engineering of Xi'an University of Technology, 2005: 13 - 17. (in Chinese)

闭式高速压力机组合机身的载荷谱分析

郑恩来　贾　方　张志胜　史金飞

(东南大学机械工程学院,南京 211189)

摘要:基于力学的基本理论对带有平衡机构的曲柄滑块机构进行运动学和动力学分析. 通过近似简化曲轴的力学模型,获得了曲轴与上横梁轴承座之间相互作用的载荷谱理论公式. 利用 Matlab 对空载和打桩 2 种工况下组合机身的载荷谱数据进行仿真,分析这 2 种工况下载荷谱曲线的规律. 仿真结果表明,在空载情形下,曲轴和上横梁轴承座之间相互作用的理论与仿真载荷谱曲线呈现周期性的正弦波形式;在打桩工况下,曲轴和上横梁轴承座之间相互作用的理论和仿真载荷谱曲线呈现周期性的脉冲波形式. 该结果能够为有限元法分析闭式高速压力机组合机身动力学性能过程中载荷的确定提供理论基础.

关键词:压力机; 载荷谱; 曲轴; 曲柄滑块机构

中图分类号:TP113. 1